Gas Atmosphere and Pore Size Distribution Effects on the Effective Thermal Conductivity of Nano-Scaled Insulations

K. Raed, G. Barth, R. Wulf, U. Gross

Institut für Wärmetechnik und Thermodynamik, Technische Universität Bergakademie Freiberg, 09596 Freiberg, Germany, email: gross@iwtt.tu-freiberg.de

Abstract

In the present contribution a number of porous materials has been investigated with various porosities (75 % < ψ < 93 %), mean pore diameters (360 < δ_{50} < 50,000 nm), and pore size distributions which are partly narrow and partly wide spread. The effective thermal conductivities have been measured between 500 and 1000 K in nitrogen, helium, argon and a nitrogen/hydrogen mixture (60/40 mol-%). Results are presented for the measured effective thermal conductivities with a strong effect of the kind of gas. For data evaluation, models available from the literature have been analyzed with respect to their ability for conductivity conversion from one gas to another. Suitable equations have been applied to the measured data, and agreement of measured and converted data has only been found in case of big sized pores. The deviations increase for smaller pore diameters and even stronger in cases of wide spread pore size distributions. A simple evaluation based on the Knudsen number corrected gas conductivity proved to be not successful in the latter case. These results are discussed in the light of the coupled effects of pore size, pore size distribution, accommodation coefficient and mean free path of the various gases.

1. Introduction

The effective thermal conductivity is one of the most important physical properties of insulating materials which are widely used in industry in various gas atmospheres. Highly porous materials are applied in order to minimize conduction heat transfer. The pore size is chosen small for best possible suppression of convection and also for further reduction of gas conduction and radiation. The remaining effective thermal conductivity of insulations is typically measured by panel-test facilities and transient

hot-wire instruments respectively which are open to the ambient, i.e. the (open) pores are filled with air. Measured data are usually adapted to the actual gas atmosphere by means of simple models considering gas thermal conductivity and porosity effects. So far the industrial practice.

Since the second decade of 20th century many mathematical models have been suggested for the prediction of the porous-media effective thermal conductivities. An early compilation is given by Russell (1935) [1] and after that huge efforts have been made for the development of models mostly fitted to experimental results, see e.g. Verschoor et al. (1952) [2], Tsao (1961) [3], Luikov et al. (1966) [4], Lal Chaurasia (1978) [5], Kamiuto et al. (1984) [6], Rath et al. (1990) [7], Litovsky and Shapiro (1996) [8], Singh (2004) [9] and others. The various models differ from each other depending on the material's structure and the contributions of the various heat transfer mechanisms to the entire heat flow, and among others the kind and state of the gas inside the pores play an important role. The motivation of the present investigation is an attempt for comparison of experimental results and respective predictions by the various models, when the gas filling the pores is varied. This is investigated and discussed in the temperature range 500 to 1000 K.

2. Experiments

2.1 Measurement of the effective thermal conductivity

The effective thermal conductivity is measured by application of a radial heat flow method (see Maglic et al, 1984 [10]). A respective test facility (RA1) has been designed and constructed as shown in fig.1. The heat flow is created inside the central heating rod made from graphite. It is transmitted in radial direction through the hollow cylindrical sample (fig.2a) and subsequently through an insulating layer, and finally it is absorbed in a cooling water system. The latter one consists of three calorimeters, with the central one applied for the heat flow measurements and the two guarding calorimeters above and below. The

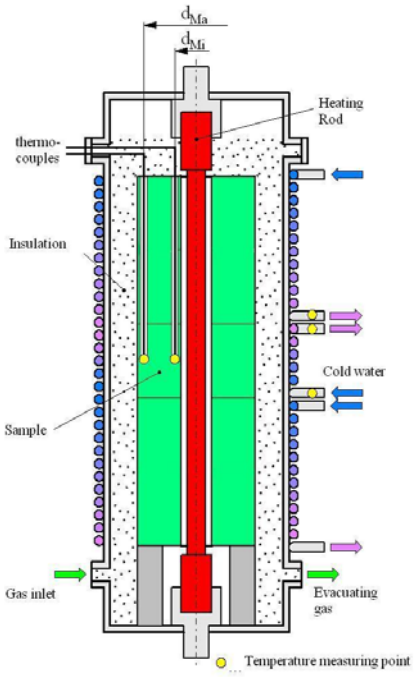

Figure 1: Schematic of experimental facility RA1

entire facility is completely encased and it can be evacuated and filled with an arbitrary but non oxidizing atmosphere. In the present experiments three pure gases (helium, argon, nitrogen) have been applied and additionally a nitrogen/hydrogen mixture (60/40 mol-%) which is of technological interest. For the gas exchange, the test facility has been thoroughly and repeatedly evacuated and filled by the respective gas.

2.2 Sample characterization

All samples (fig.2a) are prepared to be suitable for RA1 with 12 and 60 mm as the inner and outer diameter respectively and three of them are placed one on top of the other for getting a total height of 180 mm. The radial temperature differences are measured across the sample by six thermocouples equally spaced at two different diameters. In the past this apparatus has widely been tested experimentally and it has been analyzed by FEM simulations. The uncertainty of the measured effective thermal conductivities proved to be within ± 5 % [11].

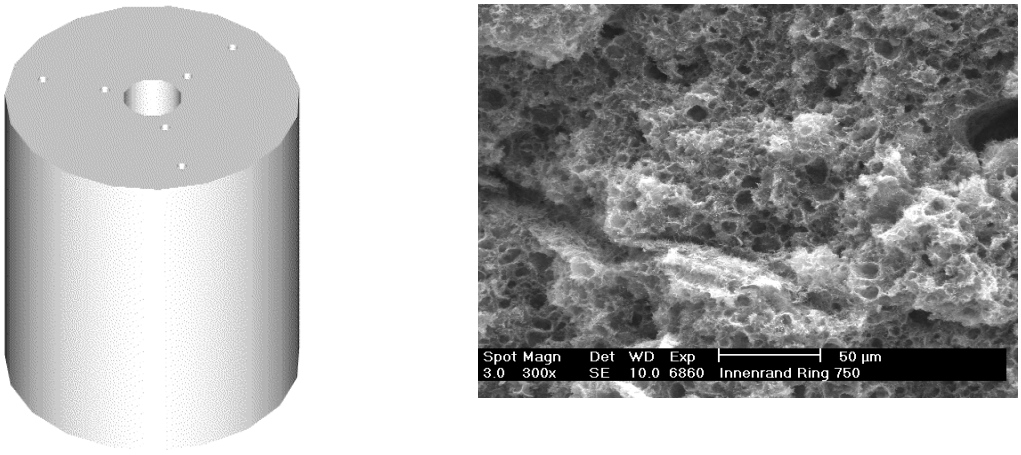

a. b.

Figure 2: (a) Sample of porous material, (b) Scanning electron microscopy image of one sample

Samples from seven different porous ceramic materials have been investigated (table 1). The selected materials have wide ranging bulk densities ($217 < \rho < 640$ kg m^{-3}) and the porosities are mostly above 90 %, except sample 6 (75.7 %). Fig.2b shows a scanning electron microscopy image of one of those samples. The pore size distributions have been determined by the mercury intrusion

porosimetry (following DIN 66133 standard [12]) which enables detection of pore sizes from the micro range (100 µm) down to diameters of 3 nm. The principle of this method is based on the intrusion of mercury into the pores by application of an external pressure where the volume of the intruded mercury is evaluated by means of a respective model to get the pore diameters.

Table 1: Listing of insulation materials, their porous structure and gas atmospheres, in which the thermal conductivity measurements were performed

Sample No.	Group No.	Solid Density [kg .m^{-3}]	Bulk Density [kg .m^{-3}]	Porosity %	δ_{10} [nm]	δ_{50} [nm]	δ_{90} [nm]	δ_{mp} [nm]	Filling gas			
									Ar	N_2	$H_2\backslash N_2$	He
1.	II	3284	217	93.4	600	460	160	7541		X	X	X
2.	III	3519	271	92.3	32900	2000	24	5097		X	X	X
3.	III	3512	306	91.3	32900	520	14	4228	X	X	X	X
4.	II	2976	273	90.8	600	560	200	8826		X	X	X
5.	III	3603	346	90.4	6000	360	14	2952	X	X	X	X
6.	I	2633	640	75.7	107340	50000	6000	-		X	X	X
7.	II	3786	261	93.1	450	420	40	8238	X	X		X

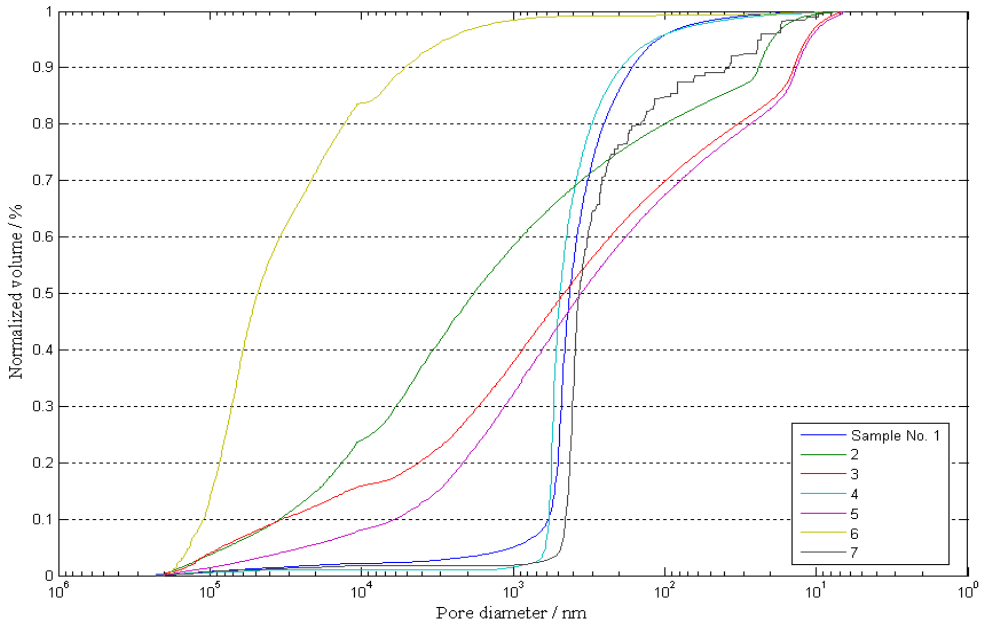

Figure 3: Pore size distributions of all samples

Fig.3 shows the pore size distributions of all samples which can be classified into 3 groups:

- Group I (sample 6): almost all of the pores are found to be micro scaled, i.e. they are big sized when compared with the other samples. Roughly 90 % of the total gas volume is enclosed in pores with diameters $\delta > \delta_{90}$ = 6,000 nm and the contribution of nano scaled pores (δ < 200 nm) is negligible. The mean diameter amounts to δ_{50} = 50,000 nm, i.e. 50 % of the volume is included in pores with $\delta > \delta_{50}$.
- Group II (samples 1, 4 and 7): here the mean diameter is much smaller (420 < δ_{50} < 560 nm) and big pores (δ > 1,000 nm) contain only a very small percentage of the total gas volume. The same is true for the nano scaled pores with only 10 % volume inside pores with δ < 200 nm (samples 1 and 4) and δ < 40 nm (sample 7).
- Group III (samples 2, 3 and 5): this group shows a completely different characteristic with wide pore size distributions having, however, δ_{50} values (samples 3 and 5) which are not far from those of group II. 30 to 40 % of the gas volume is inside pores (δ > 1,000 nm) and about 10 % inside nano scaled pores with δ < 15 nm. The characteristic of sample 2 is similar, however, somewhat shifted to larger pore diameters

Table 1 includes significant data for the description of the pore size distribution, i.e. the near maximum diameter δ_{10}, the mean diameter δ_{50}, and the near minimum one δ_{90} (with the indices 10, 50, 90 referring to the percentage of the intruded volume, there is an additional column for δ_{mp} which will be discussed later).

2.3 Experimental results

Lots of effective thermal conductivity measurements have been carried out between 500 and 1000 K with all of the seven samples in the gas atmospheres as listed in table 1. Fig.4 shows a typical result obtained for sample 3 with effective thermal conductivities which increase with the temperature and also with the kind of gas from argon to nitrogen, the nitrogen/hydrogen mixture and finally to helium. The latter increase amounts to about $\Delta\lambda_{eff} = 0.03\ W\,m^{-1}K^{-1}$ corresponding to more than 250 %

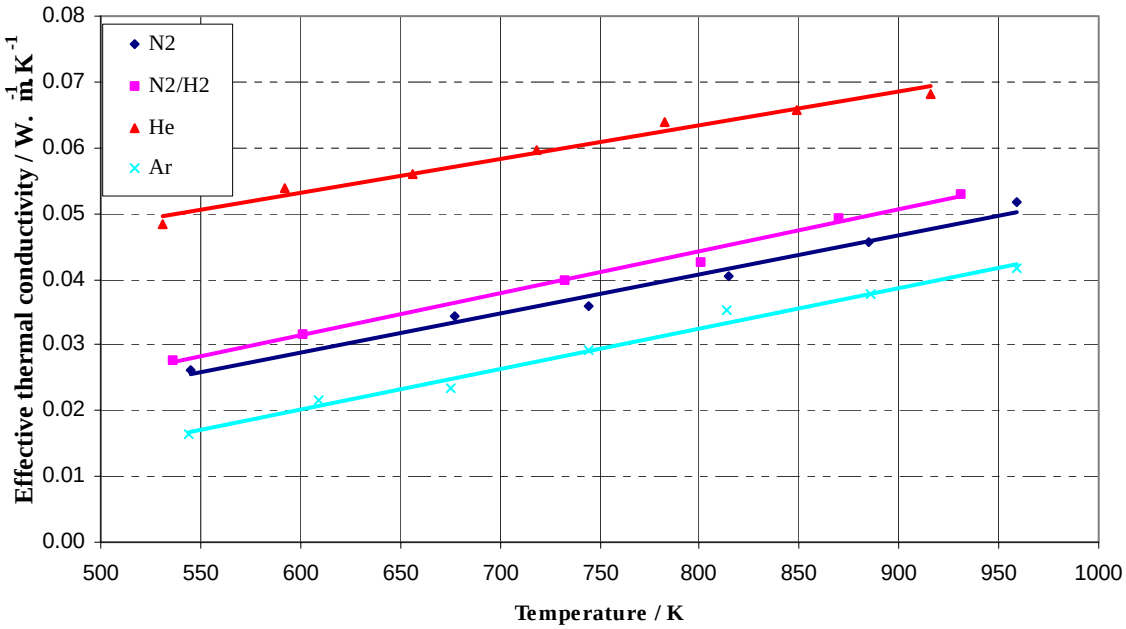

Figure 4: Results of measurements of thermal conductivity of sample No. 3 vs. temperature in different gas atmospheres

in the low temperature range. The temperature effect proves to be nearly linear and at first glance it seems to be independent of the kind of gas except the heilum results with a somewhat smaller slope. In the next step the observed variation of the effective thermal conductivity from one gas to another will be evaluated by application of physical models.

3. Data analysis

3.1 Theoretical background

Basically there are three different heat transfer mechanisms in porous media, namely conduction in solid and gas, radiation in solid and gas, and convection of the gas. Actually, the contribution of convection can be neglected due to the very small pores by which the macroscopic motion of the gases is completely suppressed. That has repeatedly been investigated and confirmed in the past and most recently by Daryabeigi (2003) [13] who measured two samples of fibrous high porosity insulations (bulk density 24 kg m^{-3}) by a guarded hot plate facility (at 300 to 1300 K) with two different heat flow directions, aligned and opposite to gravity. No difference has been found within the experimental uncertainty of ± 7.5%.

The effective thermal conductivity for highly porous media can be estimated by the following simple model, e.g. see Luu et al. (1986) [16]

$$\lambda_{eff} = \lambda_{solid} + \lambda_{gas} + \lambda_{rad} \tag{1}$$

with the conductive transport in the solid porous matrix (λ_{solid}) and in the gas filled pores (λ_{gas}) which is supplemented by the socalled radiation conductivity (λ_{rad}) with the assumptions, that (a) the gases (argon, nitrogen, helium) are non participating in the radiation process, see Jakob (1949) [14], and (b) the processes of conduction and radiation are not linked to each other. Actually eq.1 is a parallel heat flow model assuming the porosity to be close to unity. Applied to two identical samples filled with different gases, the subtraction of the respective formulations yields

$$\Delta\lambda_{eff\,(gas\,1)} - \lambda_{eff\,(gas\,2)} = \lambda_{gas\,1} - \lambda_{gas\,2}$$

and more briefly

$$\Delta\lambda_{eff} = \Delta\lambda_{gas} \tag{2}$$

where solid conduction and radiation are independent of the gas. By considering the uncertainty of the measured effective thermal conductivity to be ± 5 %, see 2.2, we get

$$(1 \pm 0.05)\lambda_{eff\,(gas\,1)} - (1 \pm 0.05)\lambda_{eff\,(gas\,2)} = \Delta\lambda_{gas}$$

and for the worst case

$$(1 \pm 0.1)\,\Delta\lambda_{eff} = \Delta\lambda_{gas} \tag{3}$$

If model eq.1 would be accepted, the effective thermal conductivity measured in various gas atmospheres is expected to vary exactly as the gas conductivities do with maximal deviations within ±10% following eq.3.

3.2 Evaluation based on bulk gas conductivities

As a first step model (eq.2) has been evaluated for all of the seven samples and for nitrogen and helium as the respective gases with the bulk gas conductivities from Rohsenow et al. (1998) [17]. As the result $\Delta\lambda_{eff}/\Delta\lambda_{BG}$ (with the subscript for the bulk gas conductivities) plotted vs. temperature (fig.5) large deviations from unity are found even if a $\pm 10\,\%$ range would be allowed for the measuring uncertainties of the RA1 facility. Sample 6 with its big sized pores brings the relatively best agreement with an underprediction of something more than 20 % at 500 K which is, however, decreasing for the higher temperatures. The effective thermal conductivities of all other samples are strongly overpredicted.

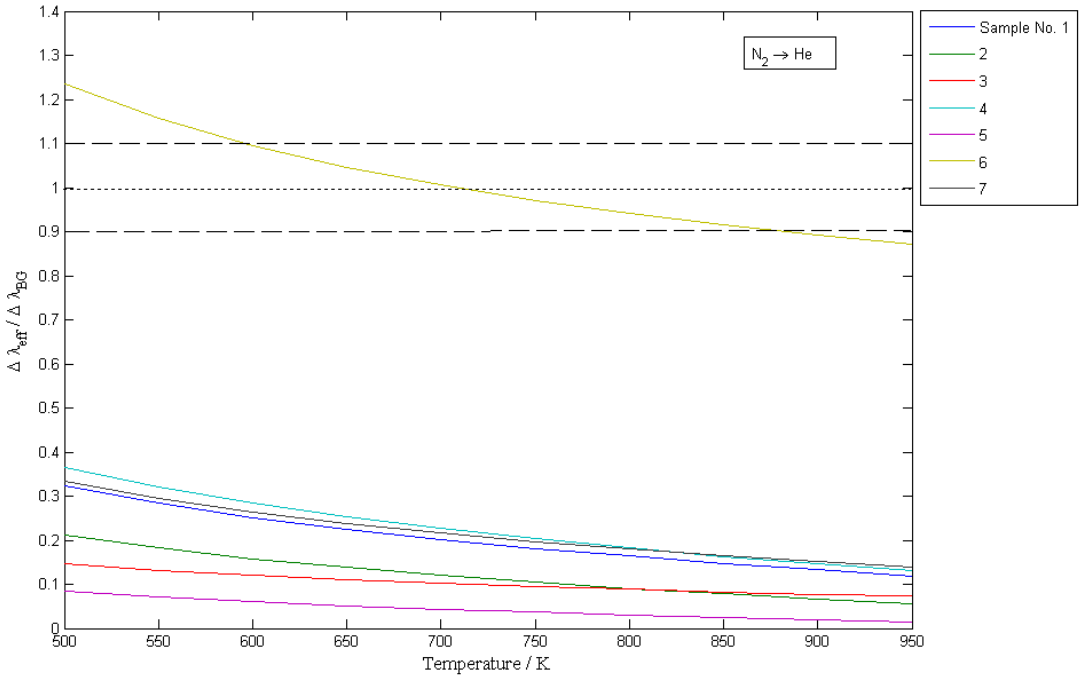

Figure 5: Results of calculation model eq.(3) based on bulk gas thermal conductivity.

On reason could be due to the porosity, which is far below unity. As expected, eqs. 1-2 simplify the problem in an unjustified way and a number of equations can be found in the literature which additionally consider porosity effects (table 2) bringing relations of the type

$$\Delta\lambda_{eff} = f(\Psi)\Delta\lambda_{gas} \qquad (4)$$

Table 2: Listing of some mathematical models of effective thermal conductivity from literature and derivated models for determination of the effective thermal conductivity variation by an exchange of the filling gas

Ref.	Model	Derivated model for exchange filling gas	Eq.-No.
[30]	$\lambda_{eff} = \Psi \cdot \lambda_{gas} + \alpha \cdot (1 - \Psi) \cdot \lambda_{solid}$	$\Delta\lambda_{eff} = \Psi \cdot \Delta\lambda_{gas}$	(5)
[6]	$\lambda_{eff} = (1 - \Psi^{2/3}) \cdot f \cdot \lambda_{solid} + \Psi^{1/3} \cdot \lambda_{gas} + \frac{16}{3\tilde{\beta}} \cdot \sigma \cdot T^3$	$\Delta\lambda_{eff} = \Psi^{1/3} \cdot \Delta\lambda_{gas}$	(6)
[7]	$\lambda_{eff} = (1 - \Psi)^2 \cdot \lambda_{solid} + \Psi \cdot (2 - \Psi) \cdot (\lambda_{gas} + \lambda_{rad})$	$\Delta\lambda_{eff} = \Psi \cdot (2 - \Psi) \cdot \Delta\lambda_{gas}$	(7)
[2]	$\lambda_{eff} = \frac{\lambda_{gas} + \lambda_{conv} + \lambda_{rad}}{\Psi} + \lambda_{solid}$	$\Delta\lambda_{eff} = \Psi^{-1} \cdot \Delta\lambda_{gas}$	(8)
[8]	$\lambda_{eff} = \lambda_{solid} \cdot M(1-\Psi)^{3/2} + \lambda_{gas}\Psi^{1/4} + \lambda_{conv} + \lambda_{rad}$	$\Delta\lambda_{eff} = \Psi^{1/4} \cdot \Delta\lambda_{gas}$	(9)

- Koglin (1967) [31], eq.5, considers the porosity effect in a parallel gas/solid heat conduction model,
- Kamiuto et al. (1984) [6], eq.6, represent the same (supplemented by radiation transport) with, however, the porosities related to the cross section instead of the volume,
- Rath et al. (1990) [7], Verschoor et al. (1952) [2] and Litovsky and Shapiro (1996) [8] have introduced porosity in more complex mathematical model eq.7-9, which fit well the experimental results of them.

These models are created from different parallel-, series-, or complex gas/solid phase distributions of the considered porous media. Respective evaluations of the eqs.5-9 bring results which again bring more or less strong deviations from the experimental findings. As an example, fig.6 shows the result evaluated from eq.5 again for nitrogen to helium. Comparing figs. 5 and 6, little has changed and again the best agreement is obtained for sample 6 with an enhanced underprediction lying between 17 and 62 % for high and low temperatures respectively. All other samples keep the overprediction

as already obtained in fig.5 which ranges from 250 % for the group II samples (1, 4, 7) up to 1000 % for samples 3, 5 (group III). These approximate deviations are valid for around 600 K increasing further with the temperature. This shows that the gas heat conduction process can only be considered to be in the free gas regime (as characterized by the bulk gas conductivity) for the big sized pores (sample 6) where, however, the strong underprediction for this low porosity sample ($\Psi = 75.7\%$) shows that the parallel heat transfer process assumed in eqs.1 and 5-9 is too simple.

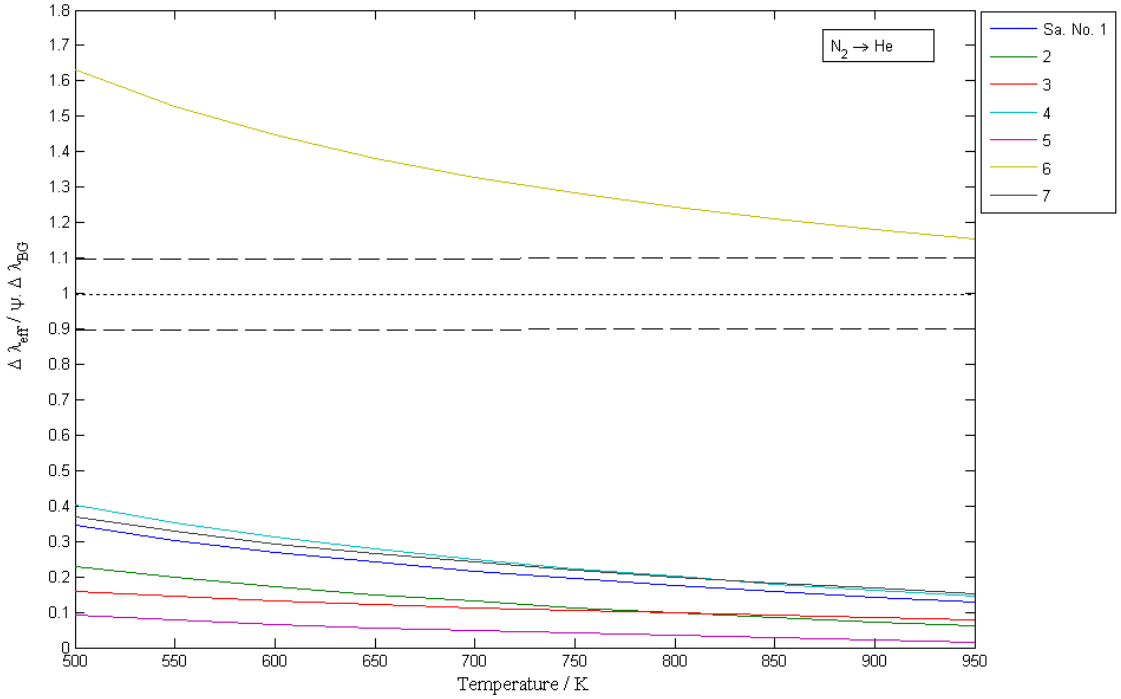

Figure 6: Results of calculation model eq.5 based on bulk gas thermal conductivity (BG).

3.3 Evaluation based on the temperature jump model

A long time ago the transport properties of a gas enclosed in very small pores has been found to be different from those in the free regime. The thermal conductivity, e.g., of the respective gas decreases below its bulk value and many attempts for its calculation have been performed, basically following two concepts. In the first one, models have been developed (e.g. by Verschoor et al. (1952) [2], Kistler (1934) [18], Woodside and Messmer (1961 [19]) for the modification of the mean free path of the gas used in the kinetic theory for the prediction of the bulk thermal conductivity. The second concept for the calculation of the gas conductivity in the pores is based on the

temperature jump model (Kennard (1938) [20]) and it is the most common used concept:

$$\lambda_{gas-p} = \frac{\lambda_o}{1 + 2\left(g \diagup \delta\right)} \tag{11}$$

$$g = \frac{2-\alpha}{\alpha}\frac{2\varepsilon}{\kappa + 1} l \tag{12}$$

where λ_{gas-p} is the gas conductivity in pores, λ_o the bulk gas conductivity, g the temperature jump, δ the mean pore diameter, α the accommodation coefficient, ε a correction constant from kinetic theory, κ the isobaric to isochoric heat capacities ratio, and l is mean free path. Eqs.11-12 have further been modified by introducing Prandtl and Knudsen numbers (Kaganer (1969) [21], Lu et al (1995) [15]).

The measured to predicted effective thermal conductivity variation ratios as shown in fig.6 has now been re-evaluated based on eqs.11-12 with the mean free path according to the kinetic theory [20] and the temperature dependent accommodation coefficients following Reiter et al. [22]:

$$\lg\left(\frac{1}{\alpha} - 1\right) = A - \frac{\frac{1000}{T} + B}{C} \tag{13}$$

with the constants A, B and C depending on the kind of gas.

Figs. 7-8 show gas and temperature effects on the evaluation of the gas thermal conductivity from eqs.11-13.

- The accommodation coefficient (fig.7a) is characterized by big differences between helium and the other two gases, all of them decreasing with rising temperatures,
- The opposite holds for the mean free path (fig.7b) and subsequently for the temperature jump (eq.12) which increases with the temperature being much larger for helium than for argon and nitrogen,
- The latter effect combined with the bulk thermal conductivity (fig.7c), both of them rising with the temperature, brings gas conductivities inside pores which may increase or decrease (fig.8, which will be discussed below).

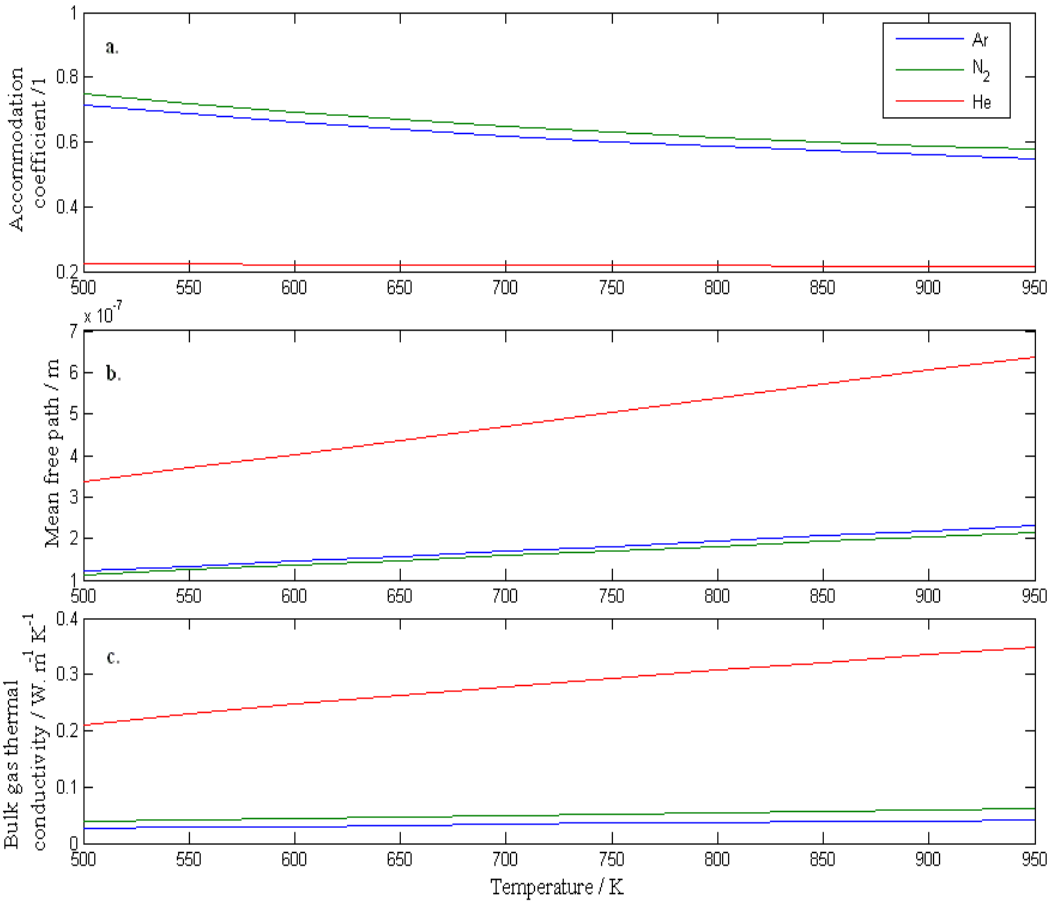

Figure 7: (a) Accommodation coefficient, (b) Mean free path and (c) bulk gas thermal conductivity for argon, nitrogen, and helium.

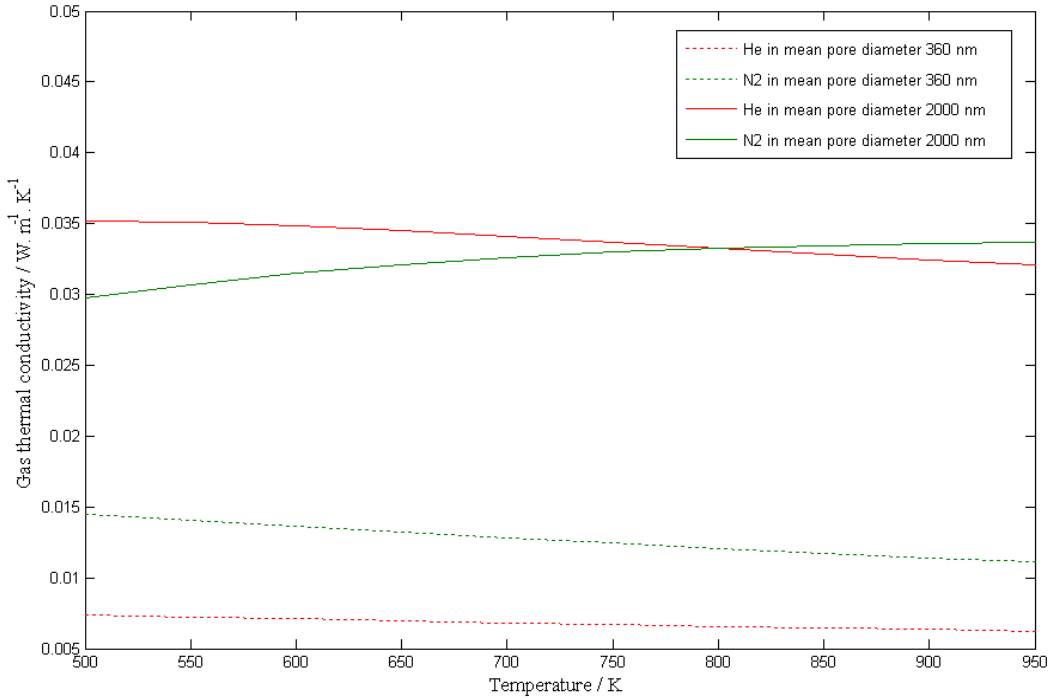

Figure 8: Variation of gas thermal conductivities with temperature for two different pore sizes depended on the jump-temperature model.

The effective thermal conductivity results evaluated again for model eq.5 and nitrogen to helium as the gases are presented in fig.9 and they are found to be very strange with partially negative data on the ordinate. A negative value of $\frac{\Delta\lambda_{eff}}{\psi\,\Delta\lambda_{gas-p}}$ means the paradoxic situation that a measured increase of the effective thermal conductivity is connected with a predicted decrease of the gas conductivity inside the pore (evaluated for the mean pore diameter according to the table 1 data). This seems to be impossible. However, what is the reason for this surprising result and what can be done for to improve it?

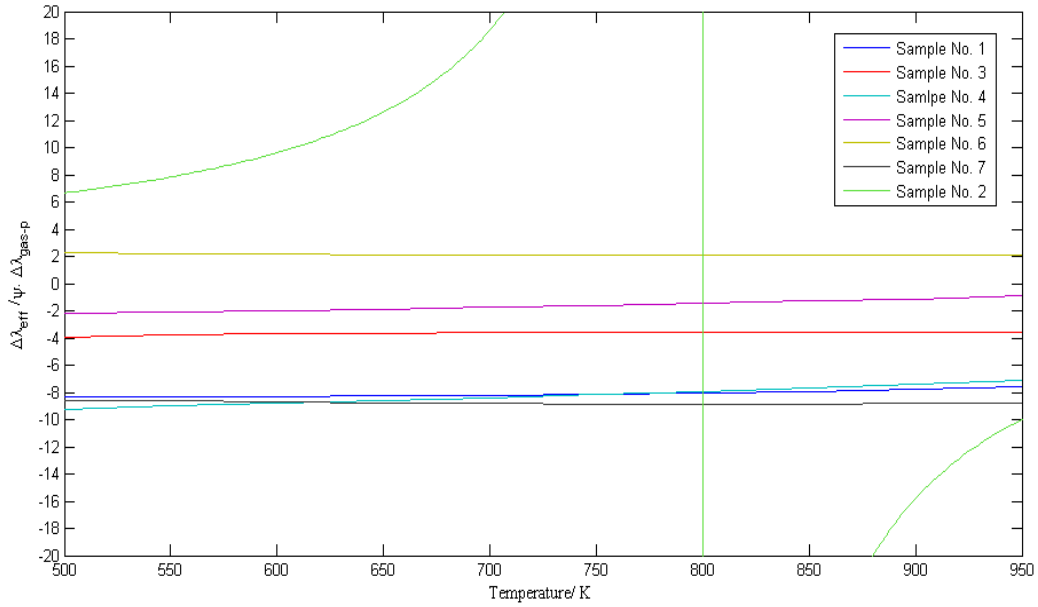

Figure 9: Results of calculations model eq.(5) based on temperature jump model.

For the reason.

The bulk conductivity of helium is much larger than that of nitrogen yielding to a respective increase of the effective thermal conductivity of a porous medium if, e.g., model eq.5 is applied. However, following eqs.11-12 the gas conductivity will decrease for both of the gases if considered in small pores and the decrease is much stronger in case of helium due to its very small accommodation coefficient as shown in fig.10 for 600 K. In small pores (about δ < 2,000 nm) the thermal conductivity of helium is found to be smaller than that of nitrogen. This holds for almost all of the samples with two exceptions: (a) the big sized pores of sample 6 (with δ_{50} = 50,000

nm) and (b) the medium sized one of sample 2 (δ_{50} = 2,000 nm) where the temperature plays a decisive role bringing a change of the sign at 800 K. This can be seen in fig.8 where the gas thermal conductivities of nitrogen and helium are plotted vs. temperature for mean pore diameters 360 nm and 2000 nm representing the group III samples 5 and 2 respectively, the latter one with the crossover as found in fig.7. Furthermore, fig.9 shows that the group II results (1, 4 and 7) are close together in contrast to the samples of group III (3, 5) with nearly the same mean pore diameter but a completely different pore size distribution (see fig.3). From this, there is a very clear effect of the pore size distribution on the results which is not considered in eqs.11-12. Zeng et al. (1994) [31] developed a gas thermal conductivity model including the pore size distribution obtained from gas adsorption-desorption measurements which has further been developed (Zeng et al. (1995) [32]) for calculations of the mean free path and subsequently the gas thermal conductivity in porous materials. However, these models bring big differences when applied to the present problem with eq.5 despite their ability for successful description of the gas thermal conductivity decrease inside pores.

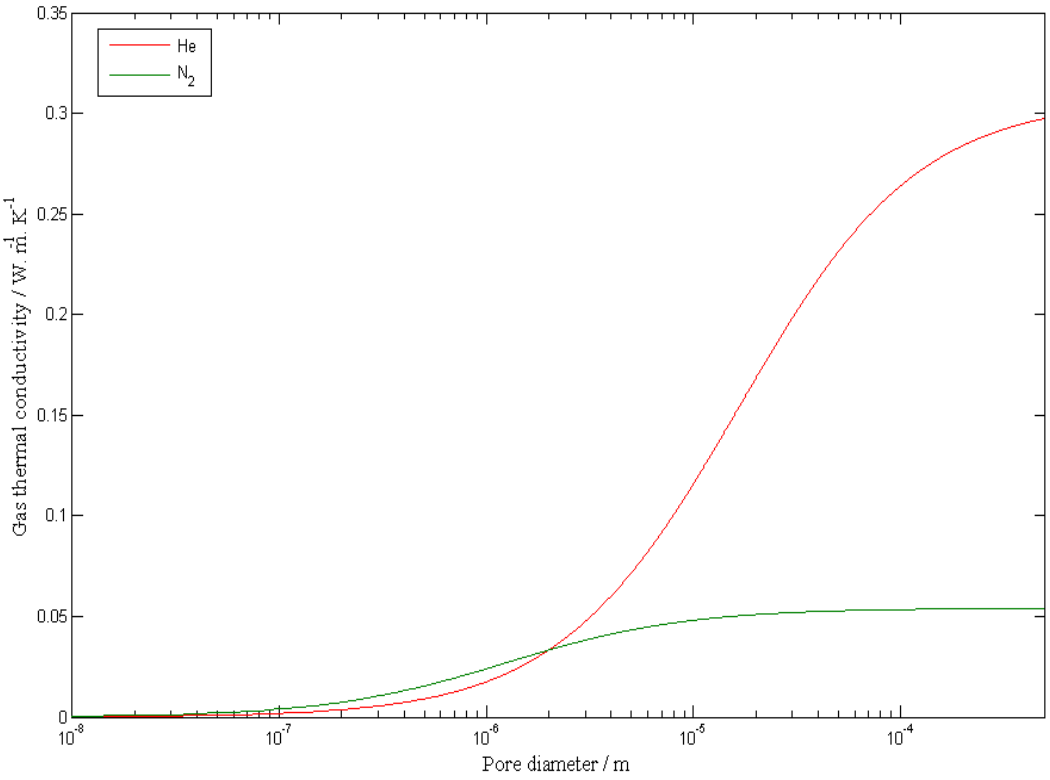

Figure 10: Changing of gas thermal conductivity for Helium and Nitrogen with pore diameter at 600 K

3.4 Evaluation for seeking a representative pore diameter

The same model eq.5 has been used with the gas conductivity from eq.11 to find the most probable pore diameter δ_{mp} of the various samples at a certain temperature (e.g. 600 K) by fitting the measured data within ± 0.1%. The result is included in table 1 and it is found to be in the micro scale being much larger than the respective mean pore diameters. For sample 6 no representative diameter can be adjusted by using the gas conductivity model eq.11 as the effective thermal conductivity is underpredicted even by application of the bulk gas conductivity (fig.5) which would have to be increased but not decreased as eq.11 does.

Now the model eq.5 is recalculated with δ_{mp} covering the entire temperature range, and as shown in fig.11 the predicted results again diverge from the measured ones as the most probable diameter depends on the temperature.

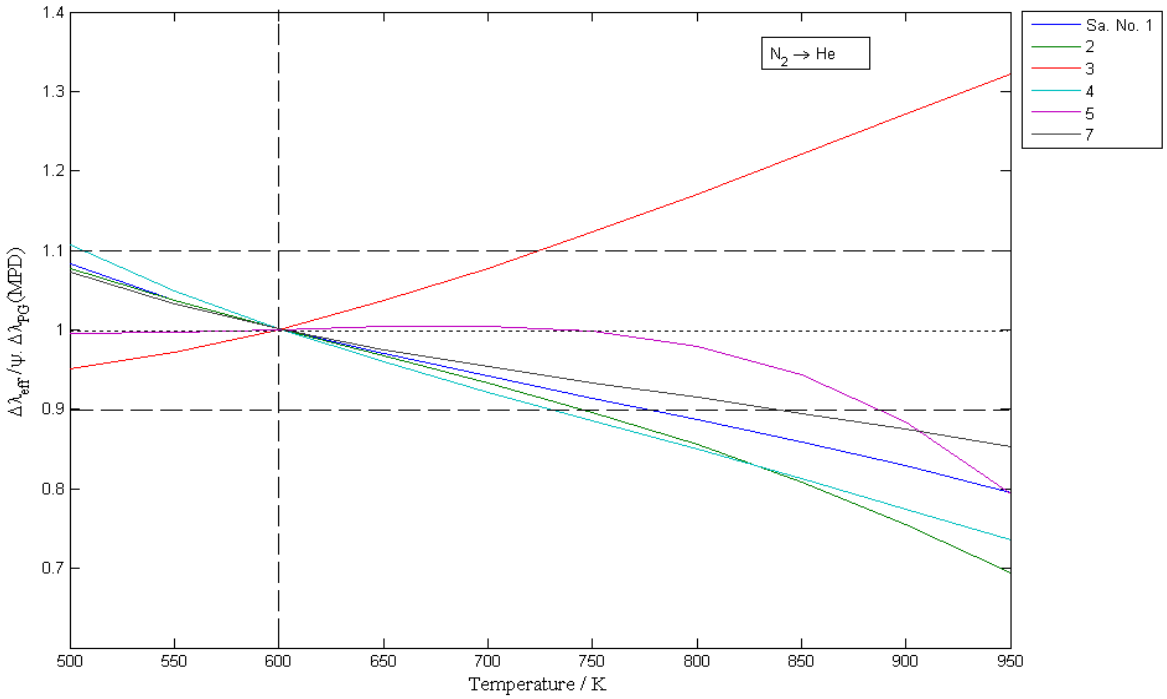

Figure 11: Results of recalculation eq.5 based on temperature jump model with most probable pore diameter.

4. Discussion:

All the various models are found to fail a proper prediction of the effective thermal conductivity, measured data could not be estimated, exchange-of-gas effects could not be calculated correctly, and there is a remaining problem for modeling the gas thermal conductivity in pores. The temperature jump model eq.9 has often been used for

modeling the gas pressure effect on effective thermal conductivity (Litovsky and Shapiro (1996) [8], Daryabeigi (2003) [13], Lu et al. (1995) [15], Wawryk and Rafaowicz (1988) [23]). This model is more commonly used than Kaganer's model (1969) [21], it has also be tested by Cunningham and Tien (1977) [24]. However, in the present investigation a big deviation from measured data has been found with increasing temperature and exchanging the gas atmosphere. Quite a number of reasons can be discussed:

(1) The present model does not consider the pore size distribution which, however, has found to be of strong influence as can seen from the various samples with similar mean pore diameter but different pore size distributions,

(2) There is a multiple temperature impact on the gas thermal conductivity, namely on the bulk conductivity, the mean free path and the accommodation coefficient,

(3) There are difficulties in the determination of the accommodation coefficient at varying temperatures: Since a long time the temperature impact on the bulk thermal conductivity is well known. Nevertheless, there are still big differences of measured results (Touloukian (1970) [25]) which is a hint to the difficulties in determination of the exact gas thermal conductivity in the bulk and in the pores respectively. In the present investigation one of the available models for the estimatation of the temperature dependent accommodation coefficient has been used. However experimental results for the accommodation coefficient (Saxena and Joshi (1989) [26]) show that accurate measurements are difficult to be estimated depending on the temperature, where the evaluated model gives decreasing accommodation coefficients with rising temperature, however in some cases it has been observed to increase (Wachman (1962) [27]). Even more, literature data are rare for all surfaces, but especially for porous insulation materials, where the accommodation coefficient is strongly related to kind and status of the surface (Wachman (1962) [27]). Wolf and Strieder (1994) [28] and Daryabeigi (1999) [33] have varied the accommodation coefficient in the range $0.01 < \alpha < 1$ for getting best fit of measured thermal conductivities to a respective model, and the accommodation coefficient for nitrogen, e.g., has found [28] to be 0.4 whereas normally a value close to unity is recommended (Reiss (2002) [30]). The

model (eq.9) contains a strong effect of the accommodation coefficient with the factor $\frac{2-\alpha}{\alpha}$ in the denominator.

(4) Difficulties in the determination of the mean free path: there are various models in the literature for the prediction bringing different results for the mean free path and subsequently for the gas thermal conductivity.

5. Conclusions

The open literature contains quite a lot of models for estimating the effective thermal conductivity which principally can be applied to predict a modification of the effective thermal conductivity of porous insulations due to the exchange of the filling gas and the respective gas conductivities. The application of all these models fails if the pores are small sized, i.e. in the range of nano scaled pores. It has been found that pore size effects upon the gas thermal conductivity has to be considered where the choice of a proper representative pore diameter proves to be a crucial problem and the pore size distribution has to be taken into account. Respective models need data like accommodation coefficient and free mean path which are only partial available in the literature and not seldom contradicting results can be found. In modeling the gas conductivity in porous media the pore size distribution has to be considered and more investigations are needed on this subject.

References:

1. H. W. Russell, Principles of Heat Flow In Porous Insulators, *J. Am. Ceram. Soc.*, **18**:1 (1935).
2. J.D. Verschoor, P. Greebler and N. J. Manville, Heat transfer by Gas Conduction and Radiation in Fibrous Insulations, *Trans. ASME* **74**:961 (1952)
3. George Tsu-Ning Tsao, Thermal conductivity of Tow-Phase Materials, *Ind. & Eng. Chem.* **53**:395 (1961).
4. A.V. Luikov, A.G. Shashkov, L. L. Vasiliey and Yu. E. Fraiman, Thermal conductivity of porous systems, *Int. J. Heat Mass transfer* **11**:117 (1966).
5. P. B. Lal Chaurasia, D. R. Chaudhary and R.C. Bhandari, Effective Thermal Conductivity to tow –Phase System, Indian *J. of Pure Appl. Phys.* **16**:963 (1978).
6. K. Kamiuto, Y. Miyoshi, I. Kinoshita and S. Hasegawa, Combined Conductive and Radiative Heat Transfer In an Optically Thick Porous Body, *Bulletin of JSME* **27**:1136 (1984).

7. D. Rath, A. Steiff and P. M. Weinspach, Zur Berechnung der effektive Wärmeleitfähigkeit von evakuierten Dämmaterialien, *Chem.-Ing.-Tech.* **62**:956 (1990).
8. E. Litovsky and M. Shapiro, Gas and temperature dependence of thermal conductivity of porous materials: Part2, Refractories and Ceramics with Porosity Exceeding 30%, *J. Am. Ceramics Soc.* **79**:1366 (1996).
9. R. Singh, Calculation of Effective Thermal conductivity of Highly Porous Two-phase Materials, *Applied Thermal Eng.* **24**:2727 (2004).
10. K.D Maglic., A. Cezairliyan and V.E. Peletsky. *Compendium of thermophysial property measurement methods*. Vol. 1 (Plenum Press, New York and London, 1984) pp. 63-67
11. Deutscher Kalibrierdienst, Angabe der Messunsicherheit bei Kalibrierungen, Technischer Bericht, *Physikalisch-Technische Bundesanstalt* (1998).
12. DIN 66 133, Bestimmung der Porenvolumenverteilung und der spezifischen Oberfläche von Feststoffen durch Quecksilberintrusion, *Deutsche Norm*, (1993).
13. K. Daryabeigi, Heat transfer in high-temperature Fibrous Insulation, *J. of Thermophysics and Heat transfer* **17**:10 (2003).
14. Max Jakob, *Heat transfer* (John Willy & Sons Inc., New York, 1949) pp.53
15. X. Lu, R. Caps, J. Fricke, C.T. Alviso und R.W. Pekala, *J. Non-Crystalline Solids* **188**:226 (1995).
16. M. Luu, B. A. Allmon, and K.E. Kneidel, *Proceeding of the international heat transfer conference, USA*, (1986), pp.709-714
17. W. M. Rohsenow, J. P. Hartnett and Y. I. Cho, *Handbook of Heat Transfer*, Third Edition (McGraw-Hill, 1998), pp. 2.1-2.11
18. S. S. Kistler, Thermal conductivity of silica Aerogel, *J. of Physical Chem*., **39**:79 (1934).
19. W. Woodside and J. Messmer, Thermal Conductivity of Porous Media. I. Unconsolidated Sands, II. Consolidated Sands, *Journal of Applied Physics* **32**:1688 (1961).
20. Earle H. Kennard, *Kinetic Theory of Gases* (McGraw-Hill, New York and London, 1938), pp.311-320
21. M. G. Kaganer, *Thermal Insulation in Cryogenic Engineering*, (Program for Scientific Translations, Jerusalem, 1969).
22. F. N. Reiter, J. Camposilvan and R. Nehern, Accommodation Coefficients of Nobel Gases on Pt-Surfaces from 80 up to 450 K, *Wärme- und Stoffübertragung* **5**:116 (1972).
23. R. Wawryk and J. Rafaowicz, The influence of residual Gas pressure on the Thermal Conductivity of Microsphere Insulation, *International Journal of Thermophysics* **9**: 611 (1988).
24. G. R. Cunnington, Jr. und C. L. Tien, Heat transfer In Microsphere Insulation In the Pressure of a Gas, *15th International Conference on Thermal Conductivity*, Ottawa (1977) pp.325-333
25. S. Touloukian, P.E. Liley, und S.C. Saxena, Thermal Conductivity Nonmetallic Liquids and Gases, *Thermophysical Properties of Matter Vol. 3* (IFI/New York, ,1970) pp.34a
26. S.C. Sexena and R. K. Joshi, *Thermal Accommodation and Adsorption Coefficients of Gases*, (Hemisphere Publishing Corp., New York, 1989), pp. 147-151.

27. Harold Y. Wachman, the Thermal Accommodation Coefficient: A Critical Survey, *ARS Journal*, 2-12 (1962).
28. Jeffrey R. Wolf and William C. Strieder; Pressure-Dependent Gas Heat transport in a Spherical pore, *AICHE Journal* **40**:1287 (1994).
29. H. Reiss, *VDI-Wärmeatlas 9*. (erweiterte Auflage), VDI-Verlag, Kap. Kf (2002).
30. B. Koglin, Der Wärmetransport in Schaumstoffen, TU Berlin, Dissertation (1967).
31. S. Q. Zeng, A. J. Hunt, W. Cao., and R. Grief, Pore Size Distribution and Apparent Gas Thermal Conductivity of Silica Aerogel, *Trans. ASME* **116**:756 (1994).
32. S. Q. Zeng, A. Hunt, and R. Grief, Mean Free Path and Apparent Thermal Conductivity of a Gas in a porous Medium, *Trans. ASME* **117**:758 (1995).
33. K. Daryabeigi, Analysis and Testing of High Temperature Fibrous Insulation for Reusable Launch Vehicles. *37th AIAA Aerospace Sciences Meeting and Exhibit January* (1999).